

Matrix Composition and Mechanics Direct Proangiogenic Signaling from Mesenchymal Stem Cells

Amr A. Abdeen, BS, Jared B. Weiss, BS, Junmin Lee, MS, and Kristopher A. Kilian, PhD

The secretion of trophic factors that promote angiogenesis from mesenchymal stem cells (MSCs) is a promising cell-based therapeutic treatment. However, clinical efficacy has proved variable, likely on account of ill-defined cell delivery formulations and the inherent complexity of cellular secretion. Here we show how controlling the mechanical properties and protein composition of the extracellular matrix (ECM) surrounding MSCs can guide proangiogenic signaling. Conditioned media from MSCs adherent to polyacrylamide hydrogel functionalized with fibronectin, collagen I, or laminin was applied to 3D matrigel cultures containing human microvascular endothelial cells (HMVECs). The degree of tubulogenesis in HMVECs is shown to depend on both the substrate rigidity and matrix protein composition. MSCs cultured on fibronectin-modified hydrogels show a stiffness dependence in proangiogenic signaling with maximum influence on tubulogenesis observed from 40 kPa conditioned media, twofold higher than commercially available cocktails of growth factors. Quantitative real-time-polymerase chain reaction reveals stiffness-dependent expression of multiple factors involved in angiogenesis that corroborate the functional tubulogenesis assay. Restricting cell spreading with micropatterned surfaces attenuates the conditioned media effects; however, small-molecule inhibitors of actomyosin contractility do not significantly reduce the functional outcome. This work demonstrates how controlling matrix rigidity and protein composition can influence the secretory profile of MSCs. Model systems that deconstruct the physical and biochemical cues involved in MSC secretion may assist in the design of hydrogel biomaterials for cell-based therapies.

Introduction

ISCHEMIC HEART DISEASE is the leading cause of human mortality globally, resulting in around 7.25 million deaths each year.¹ Treatments that promote neovascularization and angiogenesis after infarction are promising therapies for myocardial repair.^{2,3} Angiogenesis therapy often involves the direct delivery of cytokines to the site of injury to promote blood vessel formation. However, methods based on this approach often suffer from undesirable side effects, including uncontrolled and abnormal vasculature.⁴ An alternative therapy based on the delivery of autologous stem cells has emerged as one of the most promising strategies for the treatment of ischemic heart disease.⁵ Of the different cell types under investigation for treatment, mesenchymal stem cells (MSCs) are one of the most promising with 19 registered clinical trials for cardiovascular diseases.⁶

MSCs are multipotent adult stem cells of mesoderm origin. They are obtained from bone marrow or adipose tissue and have the ability to differentiate into multiple cell types.⁷ MSCs are postulated to exist as pericytes in the vasculature within tissues where they are present.^{8,9} The mechanism behind the therapeutic efficacy of MSCs is contentious.

However, there is evidence that the release of paracrine immunomodulatory and trophic molecules plays a dominant role.¹⁰ There have been reports of transdifferentiation of MSCs into cardiomyocytes¹¹ and endothelial cells^{12,13}; however, recent studies suggest limited long-term engraftment of MSCs.¹⁴ Despite early successes of MSC therapy, the complex interplay of secreted mobilizing factors, immunomodulatory molecules, and trophic molecules, and the potential for engraftment and transdifferentiation, makes the precise role of these signals in cardiac repair difficult to study.

Research efforts aimed at controlling the MSC secretome for clinical applications have explored multiple strategies, including hypoxic,^{15,16} pharmacological,¹⁷ cytokine,¹⁸ or growth factor¹⁹ preconditioning, and/or genetic manipulations.^{6,20} An important aspect of the MSC microenvironment that has been shown to influence growth and differentiation—but has been relatively unexplored in guiding the MSC secretome—is the physical characteristics of the ECM.^{21–25} It has been shown that treating matrigel cultures of HUVECs with conditioned media from MSCs cultured under tension leads to enhanced tubulogenesis and signaling through the FGFR1 pathway.²⁶ In addition, MSCs cultured on compliant

substrates show dramatic differences in interleukin-8 (IL-8) expression as substrate stiffness increases.²⁷ These reports suggest that the mechanical microenvironment surrounding MSCs can play a significant role in regulating proangiogenic signaling. In addition to mechanical properties, the composition of the matrix might have a role as well as it has been shown to influence cell spreading and MSC differentiation.^{23,25} In a recent study, the effect of matrix composition was investigated in a fibrin-based MSC–HUVEC coculture system.²⁸ This work demonstrates that the collagen/fibrin ratio can affect network formation and an inverse relation between matrix stiffness and network formation exists. While this study provides some insight into the complex interplay of ligand composition and matrix mechanics, the precise role these factors play in directing proangiogenic signaling remains to be revealed.

In this article we use a model hydrogel system, where we can independently tune matrix composition and stiffness, to investigate proangiogenic signaling from adherent MSCs. Cells cultured on fibronectin hydrogels show stiffness dependence in secretion of proangiogenic molecules as determined by monitoring tubulogenesis from endothelial cells in matrigel. Using soft lithography to restrict cell spreading, we find partial abrogation of the stiffness trend. Quantitative real-time–polymerase chain reaction (RT-PCR) reveals a complex regulation of secretory molecules from MSCs in response to substrate stiffness and matrix protein composition. The approach presented here may prove a facile method to screen for optimum conditions that promote secretion of proangiogenic factors toward the development of injectable biomaterials for cell-based regenerative therapies.

Materials and Methods

Materials

Lab chemicals were purchased from Sigma-Aldrich unless otherwise stated. Hydrazine hydrate was purchased from Fisher Scientific. Human ECM proteins (fibronectin, collagen I, and laminin α 1) were purchased from Sigma. Tissue culture plastic was purchased from Fisher Scientific. Cell culture media and reagents were purchased from Gibco. Human MSCs were purchased and tested for purity from Lonza and were positive for CD105, CD166, CD29, and CD44 and negative for CD14, CD34, and CD45 by flow cytometry. Growth-factor-reduced basement membrane extract was purchased from Trevigen. Human microvascular endothelial cells (HMVECs) were purchased from Cell Systems. Endothelial growth media-2 (EGM-2)–supplemented media was purchased from Lonza. The use of human cell lines in this work was reviewed and approved by the University of Illinois at Urbana-Champaign Biological Safety Institutional Review Board.

Polyacrylamide gel fabrication

Polyacrylamide gels were made as described previously.²⁹ Briefly, 18-mm coverslips were activated by treatment with 5% 3-aminopropyltrimethoxysilane solution followed by treatment with 5% glutaraldehyde solution. Hydrophobic slides were prepared by treatment with RainX (SOPUS). One milliliter of a mixture of acrylamide and bis-acrylamide monomers was mixed with 10 μ L ammonium persulfate

initiator and 1 μ L tetraethylmethylenediamine to make a working solution (varying acrylamide and bis-acrylamide concentrations to obtain different stiffnesses). Twenty microliters of this mixture was pipetted between the activated and hydrophobic coverslips and left to polymerize. The gels were then submerged in 1 mL of 55% aqueous hydrazine hydrate for 2 h followed by washing with glacial acetic acid and deionized water for 1 h each. Fibronectin, type I collagen, and laminin α 1 were made up to 50 μ g/mL solutions and 3.6 mg/mL sodium periodate was added for 30 min to oxidize the protein. Fifty microliters of oxidized protein was pooled onto the activated gel surfaces for 1 h. The gels were washed extensively with phosphate-buffered saline (PBS) before cell culture. Since polyacrylamide is generally non-fouling, there was no need to block the substrates for non-specific adhesion.

Soft lithography

For patterning substrates, polydimethylsiloxane (PDMS; Polysciences, Inc.) stamps were fabricated by polymerization upon a patterned master of photoresist (SU-8; MicroChem) created using UV photolithography through a laser-printed mask. Stamps featuring circular patterns of 3000 μ m² were used. Oxidized protein was pooled onto the stamp for \sim 1 h and then dried with air. The stamp was then placed face down on the activated gel surface for 30 s before removal. The gels were washed extensively with PBS before cell culture.

Fluorescent protein labeling

Fibronectin, collagen, and laminin were labeled with fluorescein isothiocyanate (FITC) using a procedure adapted from literature.³⁰ The protein to be labeled is prepared as 1 mg/mL in carbonate buffer (pH=9). A 1 mg/mL FITC solution in dimethyl sulfoxide (DMSO) is prepared and 10 μ L is added per milliliter of protein solution. The reaction is left to proceed at room temperature for 2 h in the dark and excess FITC is removed by running the reaction mixture through centrifuge filter units with a 10,000 MWCO (Millipore). Standard curves were generated using a Nanodrop nd-1000 spectrophotometer (Thermo Fisher Scientific).

Cell culture

MSCs were passaged in DMEM low-glucose media supplemented with 10% fetal bovine serum (FBS) and 1% penicillin/streptomycin. The media was changed every 4 days and the cells were passaged at around 80% confluence. HMVECs were cultured on tissue culture plastic coated with attachment factor (Life Technologies) in EGM-2 growth-factor-supplemented media. The media was changed every 4 days and the cells were passaged at around 80% confluence.

Immunofluorescence

For immunofluorescence studies, the surfaces were rinsed twice with PBS and then fixed with 4% paraformaldehyde in PBS for 20 min followed by permeabilization using 0.1% Triton X-100 for 30 min. The surfaces were blocked in 1% bovine serum albumin (BSA). 4',6-Diamidino-2-phenylindole (DAPI; 1:5000) and Alexa-Fluor 488-phalloidin (1:200) in 2% goat serum (Gibco) were used to stain for

nuclei and filamentous actin, respectively. The surfaces were imaged using a Zeiss Axiovert inverted fluorescence microscope.

Vascularization assays

Conditioned media was collected from the cultured MSCs (p2–p8) and the cells were fixed and stained by day 4. Twenty-five microliters of matrigel was pipetted into each well of a 48-well plate. The plate was then placed in the incubator for 30 min to form the gel structure. HMVECs of low passage (p2–p6) were seeded at ~15,000 cells/well. Five hundred microliters of conditioned media obtained from the gels at 4 days was added at each condition. The assay was incubated and images of the wells were taken at different time-points using a Cannon Rebel DSLR camera on an inverted microscope at 40× zoom.

For blocking experiments, vascular endothelial growth factor (VEGF) blocking antibody (R&D Systems) was added to the conditioned media right after adding the HMVECs according to the manufacturer’s instructors.

RT-PCR analysis

For PCR analysis, cells were lysed at 2 days using TRIZOL reagent (Life Technologies). RNA was isolated by chloroform extraction (Fischer) and ethanol precipitation. The amounts of RNA were normalized and then cDNA first-strand synthesis was performed with a superscript III kit (Invitrogen) as per the vendor’s instructions. For the PCR, the following primers were used (Supplementary Table S1; Supplementary Data are available online at www.liebertpub.com/tea) along with SYBR green master mix (Invitrogen) in 20 μL reactions in a real-time PCR machine (Eppendorf). The PCR results for each factor were normalized to GAPDH and then between different biological replicates the samples were normalized to the glass condition.

Protein expression analysis

Conditioned media from the human MSC cultures was separated in sodium dodecyl sulfate (SDS) polyacrylamide gels and transferred to a nitrocellulose membrane (General Electric Healthcare) in 25 mM Tris, 192 mM glycine, 0.1% SDS, and 20% methanol using a semi-dry electroblotting system (Amersham Biosciences). Membranes were blocked with 5% BSA in Tris-buffered saline (TBS; 50 mM Tris [pH 8.0] and 150 mM NaCl) for 1 h at room temperature; primary antibodies (Santa Cruz Biotechnology) were added in TBS buffer plus 0.1% Tween-20 (TBS-T) and incubated overnight at 4°C with shaking, followed by washing with TBS-T. Horseradish-peroxidase-conjugated anti-rabbit secondary antibodies (Invitrogen) were used to detect labeling of the transferred material using a substrate kit (Amresco).

Data analysis

Tube formation was quantitated using the ImageJ software (NIH). Images were converted to black and white, background subtracted, and were thresholded to identify cells. The “analyze particles” function was then used to identify tubes from isolated cells to quantitate tube area as a fraction of total area (Supplementary Fig. S1). Statistical significance was determined using ANOVA for comparing multiple groups and using two-tailed *p*-values from unpaired *t*-test for comparing two groups.

Results

Polyacrylamide gel fabrication and chemical modification

To study how the combination of matrix protein and hydrogel stiffness influences MSC adhesion and secretion, we utilized a polyacrylamide hydrogel fabrication procedure^{29,31} (Fig. 1A). Three gels of different Young’s moduli were prepared to cover a physiologically relevant range: 0.5,

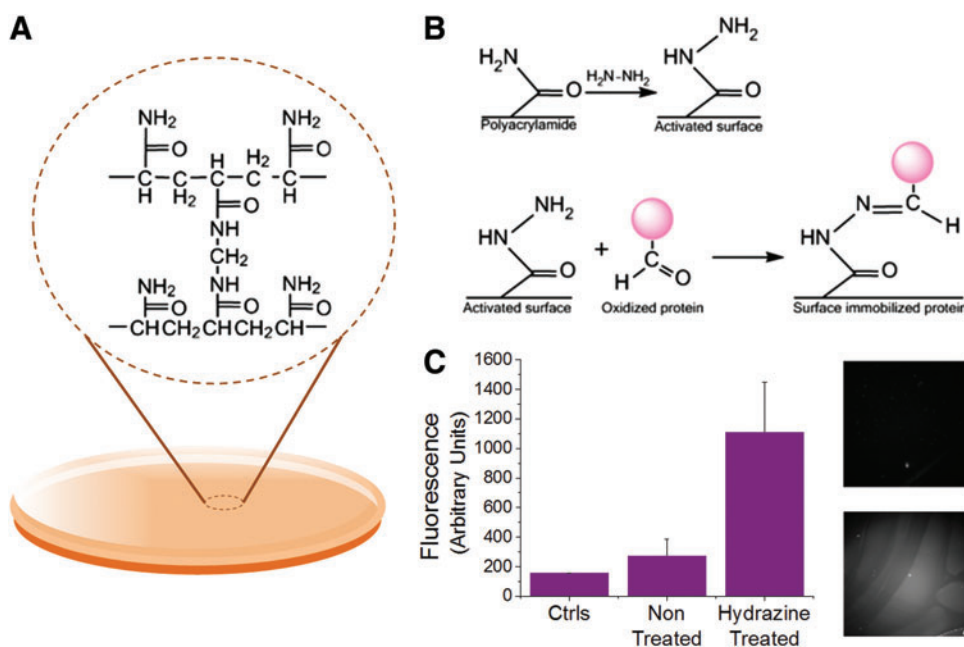


FIG. 1. Polyacrylamide gel fabrication and conjugation. (A) Polyacrylamide gel structure. (B) Hydrazine treatment of the gel surface yields hydrazide groups that react with the activated proteins to covalently attach the protein to the gel surface. (C) Left: Fluorescence measurements made with Alexa-546 fibrinogen to confirm protein immobilization. Right: Fluorescence image of non-hydrazine treated (top) versus hydrazine treated (bottom). Error bars represent standard deviation from at least three replicates (*n* = 3). Color images available online at www.liebertpub.com/tea

10, and 40 kPa. Young's moduli were confirmed using atomic force microscopy contact force measurements (data not shown). The gels were optically transparent, which is important to enable confocal immunofluorescence analysis of adherent cells. Next, we optimized a chemical modification procedure in order to covalently couple common ECM proteins to the hydrogel surfaces.²⁹ Hydrazine hydrate was applied to the hydrogels to modify the acrylamide moieties at the surface of the gel to yield distal reactive hydrazide groups (Fig. 1B). We chose matrix proteins that are common constituents in the perivascular microenvironment—fibronectin, collagen, and laminin—and oxidized the proteins using sodium periodate. Addition of the oxidized protein to the hydrogel surface leads to rapid conjugation within 1 h. To verify bioconjugation, we first mixed an Alexa-647-conjugated fibrinogen with the selected matrix protein to confirm protein conjugation and pattern fidelity as demonstrated in a previous report.³² Immunofluorescence analysis of the conjugated gels indicates higher fluorescence intensity on the gels that were treated with hydrazine, thus confirming conjugation (Fig. 1C). To ascertain the conjugation efficiency between protein and across gels of different stiffnesses, we labeled our three matrix proteins with FITC prior to oxidation. After conjugation to the surface, the raw surface fluorescence was normalized to standard curves for each fluorescence protein solution (Supplementary Fig. S2). This analysis reveals comparable protein conjugation for fibronectin, laminin, and collagen immobilized to gels of the same stiffness. However, there are significant increases in all protein conjugations as the stiffness is increased. Since stiffness is increased by changing cross-link density, it is unsurprising that the quantity of conjugated protein increases as available attachment points on the surface increase.

MSC culture on protein-functionalized gels

We next tested MSC adhesion to our protein-functionalized hydrogels. The ECM-protein-conjugated gels showed a sig-

nificantly higher degree of MSC adhesion compared with the unmodified gels, confirming the validity of our conjugation strategy. MSCs showed very different morphologies across substrates of different mechanical properties (Fig. 2A). The cells were mostly small and round on the soft, compliant substrates with many instances of two or more cells grouped together, suggesting a preference for intercellular adhesion. There were similar numbers of cells across the tested gel surfaces (Fig. 2B) while MSCs cultured on glass substrates were more numerous (Supplementary Fig. S3). The cell-projected area increased with increasing stiffness (Fig. 2C), which is consistent with literature that has demonstrated increased cell spreading with substrates of increased stiffness.^{23,33} On the intermediate 10-kPa gels, the cells were more elongated, and stress fibers appeared more coherent. On the stiffest gels, the cells show the highest spreading with the presence of a robust cytoskeleton. In our system, we noted no appreciable differences in MSC morphology across the different matrix proteins.

HMVEC culture in 3D matrigel matrices

To study the effect of conditioned media from MSCs on vessel formation, we explored a matrigel assay using human microvascular endothelial cells (HMVECs) (Fig. 3A). Cells cultured in regular EGM (negative control) had very little tube formation while cells cultured in the same media with supplemented growth factors containing a variety of proangiogenic molecules (Supplementary Table S2) had approximately threefold more tube formation (Fig. 3B). Although MSC media (supplemented with FBS) showed considerably less tube formation than the proangiogenic media containing growth factors, there was approximately twofold higher tubulogenesis than the negative control. It should be noted that MSC media had a higher amount of supplemented FBS (10%) than positive controls (2%) while negative controls had no FBS.

When comparing the MSC-conditioned media collected from the hydrogel substrates to the positive and negative

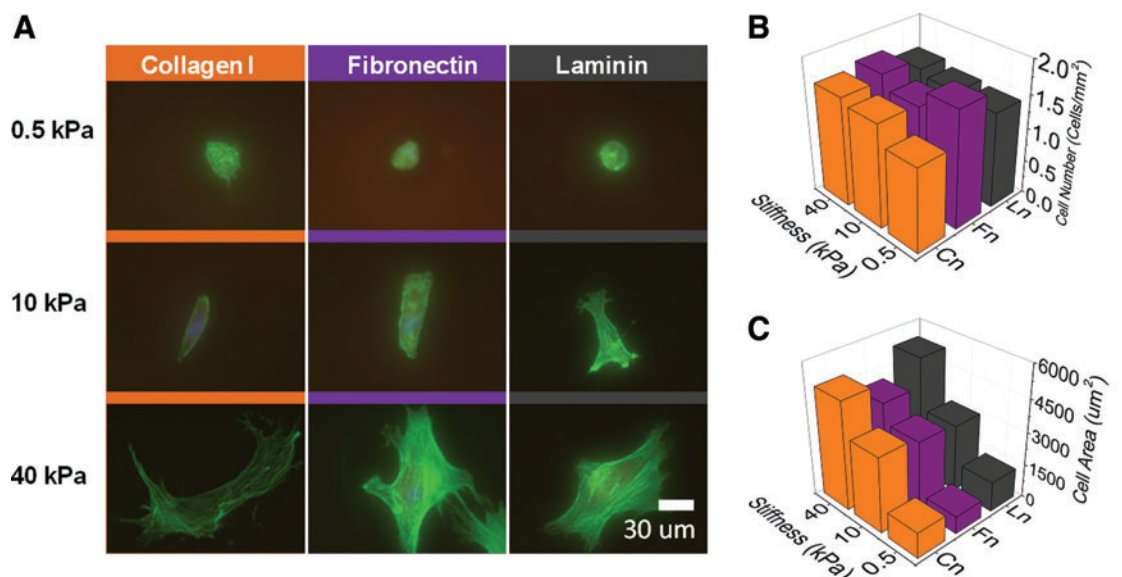


FIG. 2. Mesenchymal stem cells (MSCs) on polyacrylamide hydrogels of different stiffnesses and ligand compositions. (A) Phalloidin (green) and 4',6-diamidino-2-phenylindole (DAPI; blue) staining of MSCs on different combinations of stiffness and protein. (B) Cell numbers across the different conditions. (C) Average cell area across the different conditions. Color images available online at www.liebertpub.com/tea

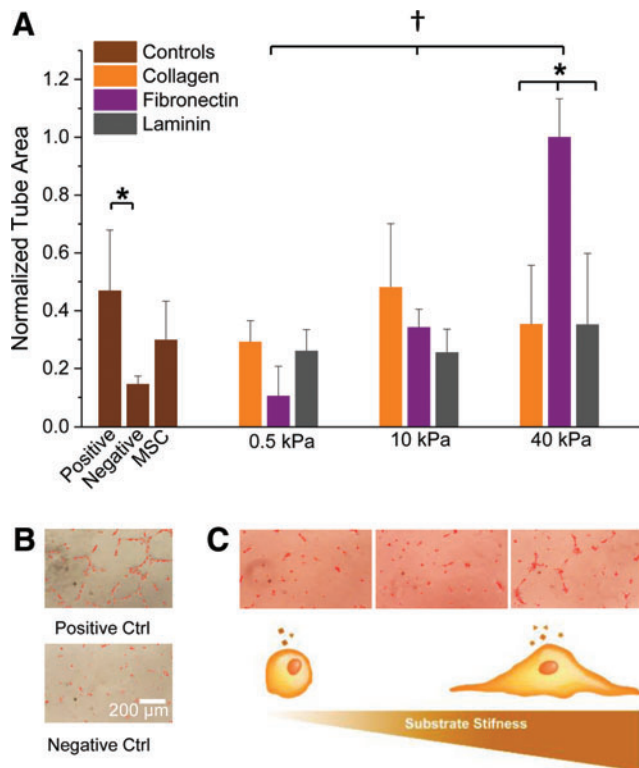


FIG. 3. Effects of MSC-conditioned media on human microvascular endothelial cell (HMVEC) tubulogenesis. **(A)** Average HMVEC tube area after treatment with conditioned media from MSCs cultured across varying stiffness hydrogels and ligand composition. **(B)** HMVECs under positive (endothelial growth media supplemented with growth factor cocktail used for HMVEC culture) and negative controls (un-supplemented media). **(C)** Top: HMVECs cultured under media from the fibronectin 0.5, 10, and 40 kPa conditions, respectively; bottom: substrate stiffness changes MSC spreading characteristics and affects their secretory profiles. Error bars represent standard deviation from three replicates ($n=3$). * $p<0.05$ and † $p<0.001$ using one-way ANOVA. Color images available online at www.liebertpub.com/tea

controls, there were subtle trends observed in the degree of tubulogenesis although not statistically significant. However, for the fibronectin condition, we observed a stiffness-dependent effect where the tube formation increases with increasing stiffness. This was not observed with the other proteins. Strikingly, the fibronectin–40 kPa condition is approximately sixfold higher than the fibronectin–0.5 kPa condition and twofold higher than the positive control containing an empirically derived cocktail of growth factors. These differences are readily apparent in the images of the HMVECs (Fig. 3C, top). The differences in tubulogenesis coincide with changes observed in MSC spreading across gels of different stiffnesses. This suggests that cell spreading—in conjunction with the composition of matrix protein—may affect the secretory profile of MSCs (Fig. 3C, bottom). To test whether cell spreading on fibronectin matrices is responsible for regulating proangiogenic signaling, we compared fibronectin-coated glass coverslips with the fibronectin–40 kPa hydrogel substrates. Interestingly, even when the number of cells is approximately sevenfold higher and the degree of spreading is higher, we see less tubulo-

genesis compared with the fibronectin–40 kPa (Supplementary Fig. S3).

Restricting cell spreading using micropatterned surfaces

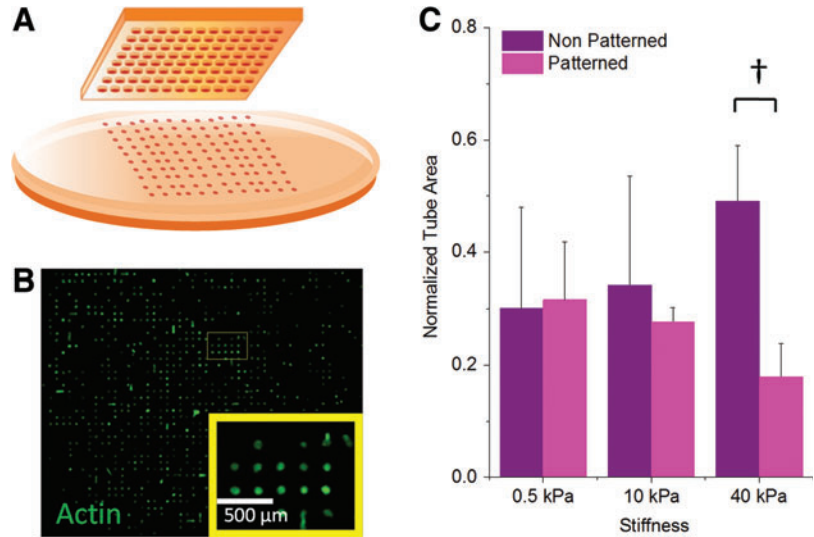
To further explore the role of cell spreading on the fibronectin-modified hydrogel substrates, we investigated the use of soft lithography to confine cells to prescribed areas across our surfaces. MSCs were captured in small fibronectin-coated islands ($3000\ \mu\text{m}^2$) across the different stiffness gels (Fig. 4A, B) and the conditioned media from these cultures was added to the HMVEC tube formation assay (Fig. 4C). Using a high-feature-density PDMS stamp for the patterned culture yields a higher number of MSCs on the patterned substrate compared with the unpatterned condition (Supplementary Fig. S4). Restricting the cells' adhesion area reduced tube formation at the fibronectin–40 kPa condition while not significantly affecting the 0.5- or 10-kPa conditions. Interestingly, the conditions with fewer cells—but with optimal spreading on 40-kPa fibronectin—lead to conditioned media that promotes enhanced tubulogenesis. Therefore, normalizing cell number across patterned and unpatterned conditions may foster an even higher functional outcome when MSCs are allowed to spread. These observations suggest that cell spread area is a factor in controlling the proangiogenic secretory properties of MSCs cultured under the fibronectin–40 kPa condition.

Increased cell spreading has been shown to increase cytoskeletal tension and influence aspects of cell fate decisions.^{21,34,35} To test whether cytoskeletal tension on account of increased spreading is responsible for enhanced secretion from cells cultured on these matrices, we added the small molecules blebbistatin and Y27632 (inhibitors of nonmuscle myosin and Rho associated protein kinase, respectively) to the adherent MSCs at concentrations that do not significantly alter cell morphology or viability. With the addition of these pharmacological modulators of actomyosin contractility to the MSCs, we do not see a statistically significant difference in the functional tubulogenesis assay (Supplementary Fig. S5).

Quantitative RT-PCR analysis of proangiogenic transcripts in MSCs on fibronectin-coated surfaces

To investigate whether the differences we observed for the fibronectin condition were due to a change in the secretory profiles of MSCs when cultured on these surfaces, we performed RT-PCR for a number of cytokines that are known to influence angiogenesis and are secreted by MSCs.³⁶ For angiogenesis promoters we selected VEGF, angiogenin, insulin-like growth factor (IGF), hepatocyte growth factor (HGF), epidermal growth factor (EGF), IL-6, and IL-8, while we selected the tissue inhibitors of metalloproteases, Timp-1, and Timp-2 as negative regulators of angiogenesis. The PCR results show that all of these factors are modulated by substrate stiffness (Fig. 5). VEGF expression increased significantly with increasing stiffness with expression in MSCs cultured on 40-kPa gels approximately threefold higher than cells cultured on 0.5-kPa gels. Interestingly, all three gel conditions show higher VEGF expression than cells cultured on glass, which suggests that physiological stiffness will elevate secretion from MSCs.

FIG. 4. MSC patterning to restrict cell area under the fibronectin condition. **(A)** Fibronectin was patterned on the surface of the gels via soft lithography with a polydimethylsiloxane stamp into $3000\ \mu\text{m}^2$ islands. **(B)** Immunofluorescence image of cells patterned on the surface of a 10-kPa gel (magnified view in inset; green—actin). **(C)** Effect of restricting cell area on HMVEC tubulogenesis. Error bars represent standard deviation from three replicates ($n=3$). $\dagger p < 0.01$. Color images available online at www.liebertpub.com/tea

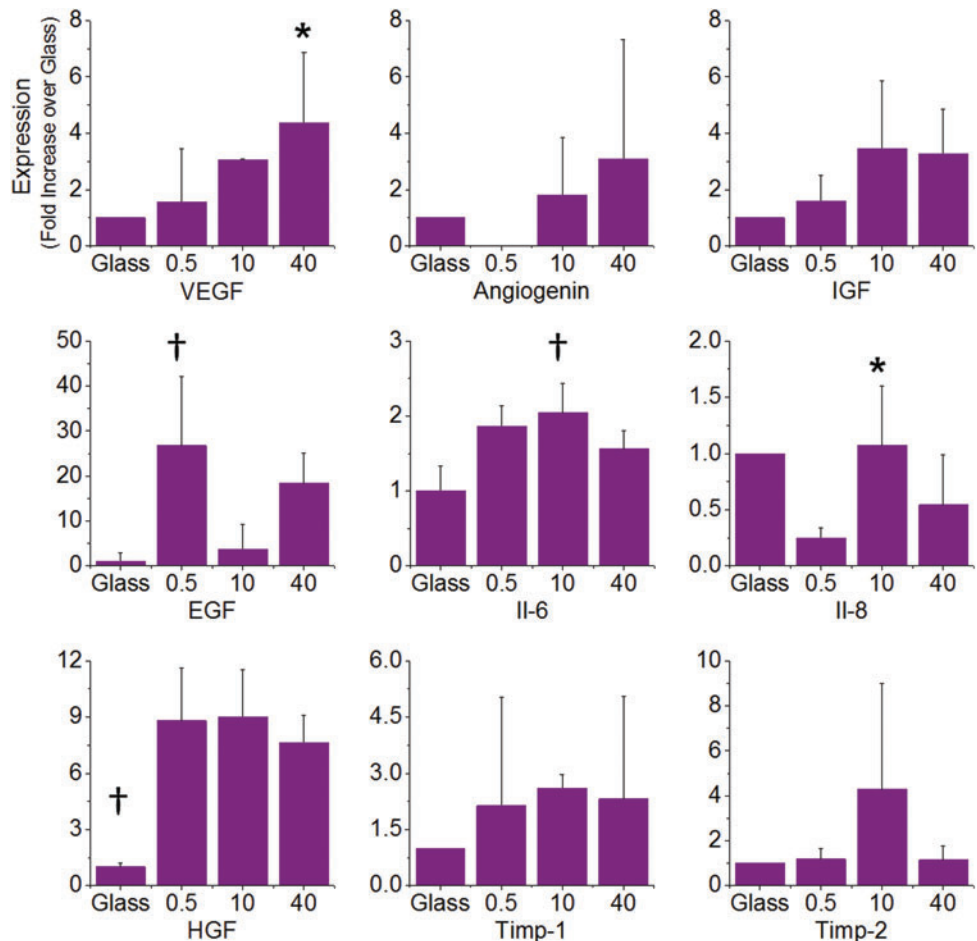


Angiogenin and IGF also show a stiffness-dependent trend in expression, which increases with gel stiffness. There was no detectable angiogenin expression for the 0.5-kPa condition. The expression of IL-6, IL-8, and EGF did not show stiffness dependence. For the angiogenesis inhibitors, Timp-1 was expressed twofold higher when cells are cultured on gels than on glass with no significant differences between the different gel conditions. Timp-2 was similar between all

conditions except the 10kPa where it was approximately fourfold higher.

From the gene expression analysis of our panel of putative angiogenesis modulators, we see differential expression depending on both stiffness and specific molecules. While regulation of angiogenesis is a complex interplay between multiple factors, we selected to inhibit VEGF as it was shown to be significantly influenced by substrate stiffness.

FIG. 5. Real-time polymerase chain reaction (RT-PCR) analysis of cytokines involved in angiogenesis. PCR shows differences in expression across different stiffnesses in vascular endothelial growth factor (VEGF), angiogenin, insulin-like growth factor (IGF), epidermal growth factor (EGF), interleukin-6 (IL-6), IL-8, hepatocyte growth factor (HGF) (promoters of angiogenesis), and Timp-1 and Timp-2 (inhibitors of angiogenesis). The results are shown as fold change relative to the glass condition. Error bars represent standard deviation from at least five replicates ($n=5$). $*p < 0.05$ and $\dagger p < 0.01$ using one-way ANOVA. Color images available online at www.liebertpub.com/tea



Blocking antibodies for VEGF were added to conditioned media prior to seeding of the HMVECs on matrigel. After quantitation, we observe no significant difference in tubulogenesis. To better discern differences between our media conditions, we performed the blocking assay with a supplement of 20% growth media that increased the degree of tubulogenesis across all MSC media conditions. Blocking VEGF in the supplemented conditioned media led to partial abrogation of the stiffness-dependent trend; however, this data is not statistically significant and merely suggests that VEGF may be one of several factors that regulate tubulogenesis in our assays (Supplementary Fig. S6).

Discussion

MSCs are an exciting cell-based therapeutic candidate for the treatment of cardiovascular disease with demonstrated clinical efficacy.³⁷ The precise role of MSCs in the healing response remains controversial but is believed to be associated with spatiotemporal secretion of molecules that reduce scarring and increase angiogenesis. Since the clinical efficacy of MSC therapy has proved variable, successful implementation of these cells will require homogenous delivery conditions that are well understood. In this article we demonstrate an approach to study the biochemical and physical properties of the ECM surrounding MSCs that guide angiogenic secretory profiles. MSCs were cultured on polyacrylamide hydrogels that are covalently conjugated with matrix proteins collagen I, laminin, and fibronectin. The choice of these proteins was guided by the *in vivo* composition of the native MSC microenvironment that is postulated to be located in the perivascular space. The adhesion and morphological characteristics of MSCs on these materials show a stiffness dependence that is in line with previous work.^{21,23,33} The cell numbers between the different conditions are comparable, which enables our empirical observations to be related to secretory effects alone. We note that while conjugation efficiency was similar across ligands, protein incorporation was higher for stiffer gels, likely due to the increased number of reactive groups as cross-link density is increased.

To study the combined role of stiffness and matrix protein on the secretory profile of MSCs, we collected conditioned media from all conditions and applied it to a model angiogenesis assay using HMVECs within matrigel. MSC-conditioned media led to enhanced tubulogenesis across all of the conditions; however, only in the case of hydrogels modified with fibronectin did we see a clear trend relating to the influence of substrate mechanical properties. Specifically, we observe an increase in tubulogenesis for HMVECs exposed to MSC-fibronectin-conditioned media where 40 kPa is always higher than the lower stiffness conditions. Interestingly, conditioned media from the fibronectin-coated glass condition—which will have a modulus on the order of GPa—shows less of a proangiogenic effect in the tubulogenesis assay. This result suggests that secretion is not only related to mechanics and there exists an optimal combination of stiffness and adhesion protein for directing proangiogenic signaling. Analogous to this finding are earlier reports that demonstrate optimal, physiologically relevant stiffness regimes for guiding MSC differentiation.^{21,23}

Previous reports have indicated that the cytoskeletal tension of MSCs can enhance secretion of paracrine fac-

tors.^{22,26} To determine whether differences in MSC spreading and actomyosin contractility across the surfaces are responsible for secretion of proangiogenic molecules, we restricted cell area using micropatterned hydrogels. Patterning MSCs in small circular islands abrogated the trend in stiffness-related secretion, giving support to the idea that cell area is implicated in controlling the angiogenic potential of these cells. However, adding drugs to inhibit actomyosin contractility (Blebbistatin; Y27632) did not cause a significant change in angiogenic potential. This suggests that although spreading plays a role in modulating angiogenic potential, actomyosin contractility is not a major factor.

To further understand MSC secretion on our protein-coated hydrogels, we performed gene expression analysis using RT-PCR of key angiogenic molecules. The proangiogenic factors VEGF, IGF, and Angiogenin show a stiffness-dependent increase in expression that correlates with the functional tubulogenesis assay results. IL-8 expression is lowest for MSCs cultured on the 0.5-kPa gel and comparable across glass, 10-, and 40-kPa conditions, which suggests that this cytokine is not involved in the observed enhancement in tubulogenesis. The expression of IL-6, HGF, EGF, and anti-angiogenesis molecules Timp-1 and Timp-2 does not show a consistent trend across these conditions; however, Timp-2 expression is low in MSCs cultured on the 40 kPa, which will assist angiogenic signaling. Importantly, the expression of VEGF, IGF, and Angiogenin in MSCs adherent to fibronectin-coated glass is negligible, further validating the result of the tubulogenesis assay. Taken together, these results show that matrix stiffness influences cytokine expression in a complex way and that the interplay of these factors leads to the final macroscopic result we see in our functional tubulogenesis assays. Since VEGF, in particular, shows a statistically significant increase in expression on the 40-kPa condition, we chose to inhibit VEGF signaling using function-blocking antibodies. VEGF blocking leads to a modest decrease in the stiffness-dependent trend in tubulogenesis, which suggests that VEGF may play a role in modulating the observed matrix effects. While the differential cytokine expression and blocking experiment provide some clues as to the role of the ECM in promoting differences in the MSC secretome, this system remains very complex, comprising many signaling molecules and intercellular signaling pathways. Future work will benefit from large-scale temporal cytokine profiling toward understanding the complex interplay between soluble factors during angiogenesis.

A caveat associated with 2D assays is that they do not fully replicate the complex signaling associated with 3D environments.^{38,39} For instance, Mooney and colleagues demonstrated 35-fold enhancement in IL-8 secretion for oral squamous cell carcinoma cells (OSCC-3) when they were cultured in 3D alginate compared with the 2D alginate surfaces.⁴⁰ MSC encapsulation within hydrogels has been shown to improve their viability during transplantation.⁴¹ Ultimately, material selection for MSC-based therapies will require 3D materials and we believe that the design parameters obtained from 2D systems such as the one described here will assist the development of more clinically efficacious 3D formulations for MSC-based therapies.

Conclusions

We demonstrate a platform to study the effect of MSC culture conditions—including matrix stiffness and adhesion protein composition—on their angiogenic potential. These physical and biochemical cues have a prominent effect on secretion, demonstrating that MSCs are sensitive to their extracellular environments. This system may prove useful as a platform for dissecting the role of material properties on the secretion of molecules from cells, and as a top-down screening method to optimize culture conditions and materials in order to attain maximum efficacy from cell-based therapies.

Acknowledgments

This work was supported by start-up funding from the Department of Materials Science and Engineering, College of Engineering at the University of Illinois at Urbana-Champaign. The authors gratefully acknowledge the support of Dr. Jennifer Amos in the Department of Bioengineering for her assistance with atomic force microscopy.

Disclosure Statement

The authors declare no conflicts of interest.

References

1. Finegold, J.A., Asaria, P., and Francis, D.P. Mortality from ischaemic heart disease by country, region, and age: statistics from World Health Organisation and United Nations. *Int J Cardiol* **168**, 934, 2012.
2. Tabibiazar, R., and Rockson, S.G. Angiogenesis and the ischaemic heart. *Eur Heart J* **22**, 903, 2001.
3. Zachary, I., and Morgan, R.D. Therapeutic angiogenesis for cardiovascular disease: biological context, challenges, prospects. *Heart* **97**, 181, 2011.
4. Epstein, S.E., Kornowski, R., Fuchs, S., and Dvorak, H.F. Angiogenesis therapy: amidst the hype, the neglected potential for serious side effects. *Circulation* **104**, 115, 2001.
5. Beohar, N., Rapp, J., Pandya, S., and Losordo, D.W. Rebuilding the damaged heart: the potential of cytokines and growth factors in the treatment of ischemic heart disease. *J Am Coll Cardiol* **56**, 1287, 2010.
6. Ranganath, S.H., Levy, O., Inamdar, M.S., and Karp, J.M. Harnessing the mesenchymal stem cell secretome for the treatment of cardiovascular disease. *Cell Stem Cell* **10**, 244, 2012.
7. Pittenger, M.F., Mackay, A.M., Beck, S.C., Jaiswal, R.K., Douglas, R., Mosca, J.D., *et al.* Multilineage potential of adult human mesenchymal stem cells. *Science* **284**, 143, 1999.
8. Crisan, M., Yap, S., Casteilla, L., Chen, C.-W., Corselli, M., Park, T.S., *et al.* A perivascular origin for mesenchymal stem cells in multiple human organs. *Cell Stem Cell* **3**, 301, 2008.
9. Da Silva, M.L., Caplan, A.I., and Nardi, N.B. In search of the *in vivo* identity of mesenchymal stem cells. *Stem Cells* **26**, 2287, 2008.
10. Ankrum, J., and Karp, J.M. Mesenchymal stem cell therapy: two steps forward, one step back. *Trends Mol Med* **16**, 203, 2010.
11. Muscari, C., Bonafé, F., Carboni, M., Govoni, M., Stanic, I., Gamberini, C., *et al.* Difluoromethylornithine stimulates early cardiac commitment of mesenchymal stem cells in a model of mixed culture with cardiomyocytes. *J Cell Biochem* **103**, 1046, 2008.
12. Wingate, K., Bonani, W., Tan, Y., Bryant, S.J., and Tan, W. Compressive elasticity of three-dimensional nanofiber matrix directs mesenchymal stem cell differentiation to vascular cells with endothelial or smooth muscle cell markers. *Acta Biomater* **8**, 1440, 2012.
13. Lozito, T.P., Kuo, C.K., Taboas, J.M., and Tuan, R.S. Human mesenchymal stem cells express vascular cell phenotypes upon interaction with endothelial cell matrix. *J Cell Biochem* **107**, 714, 2009.
14. Leiker, M. Assessment of a nuclear affinity labeling method for tracking implanted mesenchymal stem cells. *Cell Transplant* **17**, 911, 2008.
15. Kinnaird, T., Stabile, E., Burnett, M.S., Lee, C.W., Barr, S., Fuchs, S., *et al.* Marrow-derived stromal cells express genes encoding a broad spectrum of arteriogenic cytokines and promote *in vitro* and *in vivo* arteriogenesis through paracrine mechanisms. *Circ Res* **94**, 678, 2004.
16. Ohnishi, S., Yasuda, T., Kitamura, S., and Nagaya, N. Effect of hypoxia on gene expression of bone marrow-derived mesenchymal stem cells and mononuclear cells. *Stem Cells* **25**, 1166, 2007.
17. Afzal, M.R., Haider, H.K., Idris, N.M., Jiang, S., Ahmed, R.P.H., and Ashraf, M. Preconditioning promotes survival and angiomyogenic potential of mesenchymal stem cells in the infarcted heart via NF-kappaB signaling. *Antioxid Redox Signal* **12**, 693, 2010.
18. Pasha, Z., Wang, Y., Sheikh, R., Zhang, D., Zhao, T., and Ashraf, M. Preconditioning enhances cell survival and differentiation of stem cells during transplantation in infarcted myocardium. *Cardiovasc Res* **77**, 134, 2008.
19. Herrmann, J.L., Wang, Y., Abarbanell, A.M., Weil, B.R., Tan, J., and Meldrum, D.R. Preconditioning mesenchymal stem cells with transforming growth factor-alpha improves mesenchymal stem cell-mediated cardioprotection. *Shock* **33**, 24, 2010.
20. Yang, F., Cho, S.-W., Son, S.M., Bogatyrev, S.R., Singh, D., Green, J.J., *et al.* Genetic engineering of human stem cells for enhanced angiogenesis using biodegradable polymeric nanoparticles. *Proc Natl Acad Sci U S A* **107**, 3317, 2010.
21. Engler, A.J., Sen, S., Sweeney, H.L., and Discher, D.E. Matrix elasticity directs stem cell lineage specification. *Cell* **126**, 677, 2006.
22. Kilian, K.A., Bugarija, B., Lahn, B.T., and Mrksich, M. Geometric cues for directing the differentiation of mesenchymal stem cells. *Proc Natl Acad Sci U S A* **107**, 4872, 2010.
23. Rowlands, A.S., George, P.A., and Cooper-White, J.J. Directing osteogenic and myogenic differentiation of MSCs: interplay of stiffness and adhesive ligand presentation. *Am J Physiol Cell Physiol* **295**, 1037, 2008.
24. Zhang, D., and Kilian, K.A. The effect of mesenchymal stem cell shape on the maintenance of multipotency. *Biomaterials* **34**, 3962, 2013.
25. Lee, J., Abdeen, A.A., Zhang, D., and Kilian, K.A. Directing stem cell fate on hydrogel substrates by controlling cell geometry, matrix mechanics and adhesion ligand composition. *Biomaterials* **34**, 8140, 2013.
26. Kasper, G., Dankert, N., Tuischer, J., Hoeft, M., Gaber, T., Glaeser, J.D., *et al.* Mesenchymal stem cells regulate angiogenesis according to their mechanical environment. *Stem Cells* **25**, 903, 2007.

27. Seib, F.P., Prewitz, M., Werner, C., and Bornhäuser, M. Matrix elasticity regulates the secretory profile of human bone marrow-derived multipotent mesenchymal stromal cells (MSCs). *Biochem Biophys Res Commun* **389**, 663, 2009.
28. Rao, R.R., Peterson, A.W., Ceccarelli, J., Putnam, A.J., and Stegemann, J.P. Matrix composition regulates three-dimensional network formation by endothelial cells and mesenchymal stem cells in collagen/fibrin materials. *Angiogenesis* **15**, 253, 2012.
29. Damljanovic, V., Christoffer Lagerholm, B., and Jacobson, K. Bulk and micropatterned conjugation of extracellular matrix proteins to characterized polyacrylamide substrates for cell mechanotransduction assays. *Biotechniques* **39**, 847, 2005.
30. Hoffmann, C., Leroy-Dudal, J., Patel, S., Gallet, O., and Pauthe, E. Fluorescein isothiocyanate-labeled human plasma fibronectin in extracellular matrix remodeling. *Anal Biochem* **372**, 62, 2008.
31. Tse, J.R., and Engler, A.J. Preparation of hydrogel substrates with tunable mechanical properties. *Curr Protoc Cell Biol* **Chapter 10**, Unit 10.16, 2010.
32. Tseng, Q., Wang, I., Duchemin-Pelletier, E., Azioune, A., Carpi, N., Gao, J., *et al.* A new micropatterning method of soft substrates reveals that different tumorigenic signals can promote or reduce cell contraction levels. *Lab Chip* **11**, 2231, 2011.
33. Pelham, R., and Wang, Y. Cell locomotion and focal adhesions are regulated by substrate flexibility. *Proc Natl Acad Sci U S A* **94**, 13661, 1997.
34. McBeath, R., Pirone, D.M., Nelson, C.M., Bhadriraju, K., and Chen, C.S. Cell shape, cytoskeletal tension, and RhoA regulate stem cell lineage commitment. *Dev Cell* **6**, 483, 2004.
35. Gilbert, P.M., Havenstrite, K.L., Magnusson, K.E.G., Sacco, A., Leonardi, N.A., Kraft, P., *et al.* Substrate elasticity regulates skeletal muscle stem cell self-renewal in culture. *Science* **329**, 1078, 2010.
36. Skalnikova, H., Motlik, J., Gadher, S.J., and Kovarova, H. Mapping of the secretome of primary isolates of mammalian cells, stem cells and derived cell lines. *Proteomics* **11**, 691, 2011.
37. Samper, E., Diez-Juan, A., Montero, J.A., and Sepúlveda, P. Cardiac cell therapy: boosting mesenchymal stem cells effects. *Stem Cell Rev* **9**, 266, 2013.
38. Huebsch, N., Arany, P.R., Mao, A.S., Shvartsman, D., Ali, O.A., Bencherif, S.A., *et al.* Harnessing traction-mediated manipulation of the cell/matrix interface to control stem-cell fate. *Nat Mater* **9**, 518, 2010.
39. Baker, B.M., and Chen, C.S. Deconstructing the third dimension: how 3D culture microenvironments alter cellular cues. *J Cell Sci* **125**, 3015, 2012.
40. Fischbach, C., Kong, H.J., Hsiong, S.X., Evangelista, M.B., Yuen, W., and Mooney, D.J. Cancer cell angiogenic capability is regulated by 3D culture and integrin engagement. *Proc Natl Acad Sci U S A* **106**, 399, 2009.
41. Aguado, B.A., Mulyasmita, W., Su, J., Lampe, K.J., and Heilshorn, S.C. Improving viability of stem cells during syringe needle flow through the design of hydrogel cell carriers. *Tissue Eng Part A* **18**, 806, 2012.

Address correspondence to:

Kristopher A. Kilian, PhD

Department of Materials Science and Engineering

University of Illinois at Urbana-Champaign

1304 W. Green Street

Urbana, IL 61801

E-mail: kakilian@illinois.edu

Received: October 22, 2013

Accepted: April 2, 2014

Online Publication Date: May 9, 2014